



## Study of CoFeSiB glass-covered amorphous microwires under applied stress

M. Carara, K. D. Sossmeier, A. D. C. Viegas, J. Geshev, H. Chiriac, and R. L. Sommer

Citation: [Journal of Applied Physics](#) **98**, 033902 (2005); doi: 10.1063/1.1999036

View online: <http://dx.doi.org/10.1063/1.1999036>

View Table of Contents: <http://scitation.aip.org/content/aip/journal/jap/98/3?ver=pdfcov>

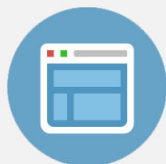
Published by the [AIP Publishing](#)

---



## Re-register for Table of Content Alerts

Create a profile.



Sign up today!



# Study of CoFeSiB glass-covered amorphous microwires under applied stress

M. Carara,<sup>a)</sup> K. D. Sossmeier, and A. D. C. Viegas

*Departamento de Física, Universidade Federal de Santa Maria, 97105-900 Santa Maria RS, Brazil*

J. Geshev

*Instituto de Física, Universidade Federal do Rio Grande do Sul (UFRGS)-Avenida Bento Goncalves 9500, C.P. 15051, 91501-970, Porto Alegre, Rio Grande do Sul, Brazil*

H. Chiriac

*National Institute and Development for Technical Physics, 47 Mangeron Boulevard 6600, Iasi 3, Romania*

R. L. Sommer

*Departamento de Física, Universidade Federal de Santa Maria, 97105-900 Santa Maria RS, Brazil and Centro Brasileiro de Pesquisas Físicas, Rua Xavier Sigaud 150 Urca, 22290-180 Rio de Janeiro RJ, Brazil*

(Received 5 November 2004; accepted 18 June 2005; published online 4 August 2005)

Magnetoimpedance-based ferromagnetic resonance (FMR) studies of annealed  $\text{Co}_{68.15}\text{Fe}_{4.35}\text{Si}_{12.5}\text{B}_{15}$  glass-covered amorphous microwires under stress are reported. The applied stress modifies the anisotropy and the domain structure present in each sample, in such a way that it can be studied through magnetoimpedance measurements and FMR dispersion relations extracted from them. From the fitting of the FMR dispersion relations, the magnitude and the orientation of the transverse anisotropy field, as well as an insight on the micromagnetic structure of glass-covered microwires, were obtained. From these studies, it can be concluded that a longitudinal anisotropy dominates the microwire behavior under zero stress. By applying an increasing stress to the microwires, an inner core with a longitudinal anisotropy surrounded by an outer shell with a circumferential anisotropy develops and dominates its magnetic behavior. © 2005 American Institute of Physics.

[DOI: 10.1063/1.1999036]

## I. INTRODUCTION

The investigation of the physical properties of glass-covered microwires has gained a great deal of attention over the past years in view of their use as sensor elements as well as to the possibility of tailoring their magnetic properties by annealing and/or applying stress (see, e.g., Ref. 1 and the references therein). Microwires are particularly suitable for use in magnetoimpedance-based sensors due to their soft magnetic properties and reduced dimensions. Glass-covered microwires present some intrinsic difficulties to be characterized due to the glass cover. On the other hand, the magnetoimpedance (MI) effect itself has been proved to be a powerful tool to investigate the magnetic properties and domain structure in magnetic materials.<sup>2-4</sup> In particular, at high probe current frequencies, ferromagnetic resonance (FMR) can be observed in the impedance spectra, improving the capabilities of extracting micromagnetic parameters from magnetoimpedance measurements.<sup>4</sup>

The aim of the present study is to investigate the magnetic properties of Co-based glass-covered microwires with vanishing magnetostriction under external stress prior to and after annealing (Joule heating) in order to control both the frozen stress level and the effective anisotropy. Besides a desirable improvement on the MI ratio  $\{\text{MI}=100 \times [Z(H$

$-Z(H_{\text{max}})]/Z(H_{\text{max}})\}$ , the main goal of this work is to investigate and control the effects of the stress and annealing on the magnetic properties, anisotropy, and domain structure of the samples by using the MI/FMR and magnetization measurements.

## II. EXPERIMENT

Glass-covered microwires with nominal composition  $\text{Co}_{68.15}\text{Fe}_{4.35}\text{Si}_{12.5}\text{B}_{15}$  were produced by the Taylor-Ulitovki technique with an amorphous nucleus of  $\phi_m \cong 25 \mu\text{m}$  and a total diameter of  $\phi_l \cong 44 \mu\text{m}$ . The samples were treated by Joule heating under 16.5 and 27.3 mA dc for 20 min in order to produce a stress relief (and anisotropy change) relative to the as-cast samples. The corresponding annealing temperatures were estimated to be 150 and 250 °C, respectively, by applying the calculation procedure described in Ref. 5. The annealing is sufficient to stabilize the magnetic parameters such as coercive and anisotropy fields.<sup>6,7</sup>

The impedance spectra  $Z(f, H)$  were measured with a HP4396B spectrum-impedance analyzer and HP4396A1 impedance test kit in the frequency range of  $100 \text{ kHz} \leq f \leq 1.8 \text{ GHz}$ . A 0 dBm (1 mW) constant power was applied to each sample, while an external magnetic field provided by a compensated coil was swept in the  $-400 \leq H \leq +400 \text{ Oe}$  range.

For the present studies a coaxial sample holder has been used, with the sample (16 mm in length) replacing the central

<sup>a)</sup>Author to whom correspondence should be addressed; electronic mail: carara@smail.ufsm.br

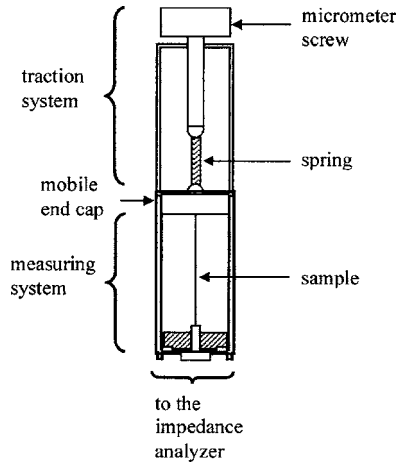


FIG. 1. Cross view of the experimental setup for the impedance measurements showing the tracking system.

conductor. At one end of the sample holder, a fixture to apply stress ( $0 \leq \sigma \leq 90$  MPa) composed of a nonmagnetic spring and a micrometer screw was attached. The applied stress was calculated as the ratio between the applied force and the sample cross section, including the glass cover. The sample holder/traction-fixture setup is schematically shown in Fig. 1. The real ( $R$ ) and imaginary ( $X$ ) parts of  $Z$  were simultaneously measured, at a given axial magnetic field, after a careful compensation of the whole fixture. From each impedance spectrum, the resonance frequency ( $f_r$ ) is obtained, as described in Ref. 4. Magnetization measurements were carried out with a Helmholtz-coil-based vibrating sample magnetometer (VSM) with a maximum magnetic field of 160 Oe applied along the wire axis with zero applied stress.

All measurements were made at room temperature.

### III. RESULTS

#### A. Magnetization

The hysteresis loops for the as-cast and annealed (250 °C) samples are shown in Fig. 2. The curves for the samples annealed at 150 °C are very similar to the as-cast ones, with a coercive field ( $H_c$ ) around 0.20 Oe and remanence ratio ( $M_r/M_s$ ) around 0.75. In view of that, only the data relative to the as-cast and annealed at 250 °C samples will be shown and discussed thereafter. For the sample annealed at 250 °C, a small increase in the saturation field was

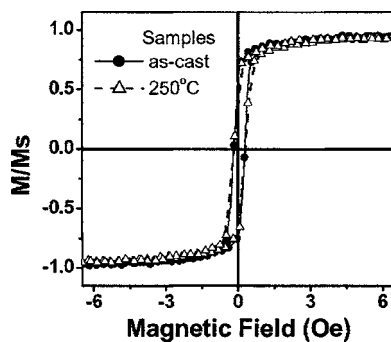


FIG. 2. Magnetization hysteresis loop of the as-cast and annealed (at 250 °C) microwires.

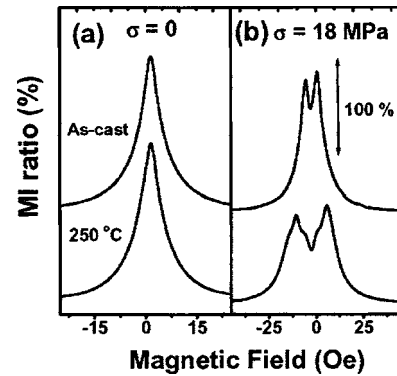


FIG. 3. Representative magnetoimpedance curves of the studied samples measured at 11.5 MHz: (a) zero applied stress and (b)  $\sigma=18$  MPa. For clarity, only the increasing field branches are shown.

observed. At first glance, all magnetization curves indicate a predominant longitudinal anisotropy. This finding seems to be in contradiction to what is expected for the domain structure in these slightly negative magnetostrictive microwires: a core-shell structure, with an axially magnetized inner core (IC) surrounded by an outer shell (OS) with a circumferential magnetization.<sup>1,2</sup> The magnetization of the OS proceeds, in general, by coherent rotation, identified in the magnetization curves by a nearly linear and reversible response. As seen from Fig. 2, either the circumferential domains are not present in the studied samples or their relative volume is very small. Such hypothesis is confirmed by the MI measurements, as discussed below.

#### B. Magnetoimpedance

In Fig. 3, the magnetoimpedance curves for the as-cast and 250 °C annealed samples are shown for zero stress and 18 MPa. At zero stress, the samples present a very similar behavior, typical of a material with a longitudinal anisotropy. For frequencies lower than the ferromagnetic resonance ( $f_r$ ) one, as shown in Fig. 3, the MI curves present just one peak (for clarity, only the field increasing branch is shown in this figure for each sample). Although the obtained MI values were high, these results will not be discussed here as this paper is mainly concerned with the effect of the annealing and stress on the micromagnetic structure of these wires.

When stress is applied, the MI behavior is drastically changed, as seen in Fig. 3(b), where the MI curves for the same frequencies used in Fig. 3(a) are shown. The absence of an OS in the as-cast sample, as proposed above, is confirmed by the single peaks centered at  $H=0$  in Fig. 3(a). As the stress is applied, a transverse anisotropy clearly develops in both samples as depicted from the double peak structure exhibited on the MI curves. A yet richer peak structure is presented by the MI curves for the sample annealed at 250 °C, the  $MI \times H$  curve still exhibiting a transverse anisotropy character. These features in the MI curves will be discussed below.

#### C. FMR dispersion relations

##### 1. Zero stress

The FMR dispersion relations for the samples measured under zero stress are shown in Fig. 4. From this figure, the

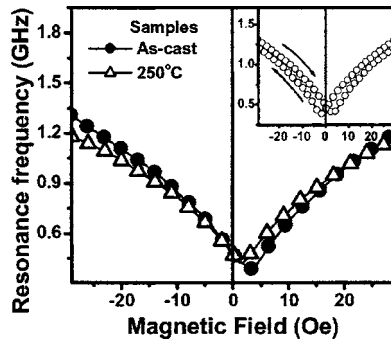


FIG. 4. FMR dispersion relation for the three studied samples with zero applied stress. The inset shows the hysteresis observed in all measured FMR dispersion curves.

longitudinal character of the effective anisotropy can be identified from the minimum in the resonance frequency at  $H \sim 0$ . As it is well known,<sup>8,9</sup> the minimum  $f_r$  for a material with longitudinal anisotropy occurs when the volume probed by the ac field is in the demagnetized state, which explains the shift from zero applied field. This situation is attained when the volume, limited by the skin depth, is demagnetized. In fact, the coercive field of the layer effectively sensed by the probe current is higher than that of the inner portion of the wire. This occurs because the magnetization of the external layer is pinned by the roughness between the metal and the glass cover. The volume sensed by the probe current is about 4% of the total wire volume, as can be inferred from the skin depth presented in Fig. 7 (see discussion below) and from the fact that the saturation field (Fig. 2) is about 3 Oe, larger than the bulk  $H_c$ . The inset in Fig. 4 presents the field-up and field-down branches of the FMR dispersion relation for the as-cast sample. A hysteresis is clearly seen in this curve. It must be noted that if only a field-up curve (from 0 to  $H_{\max}$ ) was measured, an inaccurate conclusion about the anisotropy of that sample would be drawn.

## 2. Applied stress

In Figs. 5 and 6, the dispersion relations for the as-cast and annealed samples under stress are shown. In both figures, the resonance frequency axis (y axis) is shifted for each curve for the sake of clarity.

The effect of the applied stress is to change the anisotropy axis from longitudinal to transverse, as clearly seen in the FMR dispersion relation curve of Fig. 5 for the as-cast sample. The dashed line follows roughly the evolution of the transverse anisotropy field. This increase in the transverse anisotropy field is expected for a sample with a negative magnetostriction. A similar trend can be observed in Fig. 6 for the sample annealed at 250 °C. In this case, however, two distinct anisotropy fields (indicated by the dashed lines) seem to be present for higher stress values.

## IV. DISCUSSION

In what follows, the above results will be analyzed by taking into consideration (a) the skin depth ( $\delta_m$ ) which defines the sample's volume effectively sensed by the ac probe current, and (b) the stress distribution in the wire.

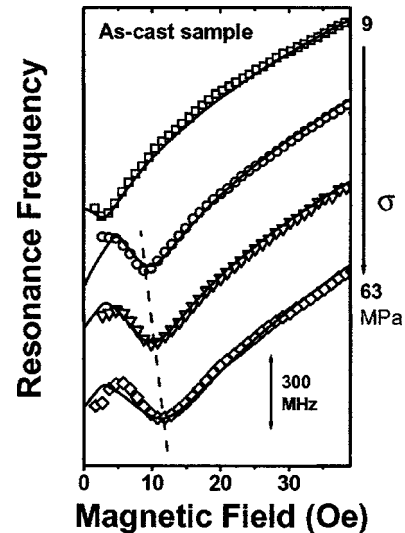


FIG. 5. FMR dispersion relation of the as-cast sample with applied stress. The symbols ( $\square$ ) 9, ( $\circ$ ) 36, ( $\triangle$ ) 54, and ( $\diamond$ ) 63 MPa represent the experimental data, and the curves are the corresponding fittings. The dashed line roughly follows the anisotropy field.

In a first approximation,  $\delta_m$  can be estimated using the value of the measured ac resistance and its variation with the frequency of the probe current. More specifically, current flows through the effective cross section, which is limited by the skin depth that decreases when the frequency and/or the transverse permeability increase. For high frequencies (such that FMR is present) and high permeabilities (such as  $\delta_m \ll \phi_m$ ),  $\delta_m$  can be approximated by

$$\delta_m = \frac{R_{dc}\phi_m}{4\text{Re}[Z(H,f)]}, \quad (1)$$

where  $R_{dc}$  is the dc value of the resistance and  $\text{Re}[Z(H,f)]$  is the ac resistance of the sample at magnetic field  $H$  and probe current frequency  $f$ . The  $\delta_m$  values calculated for  $H=0$  at the FMR frequency are shown in Fig. 7. As it can be seen,  $\delta_m$

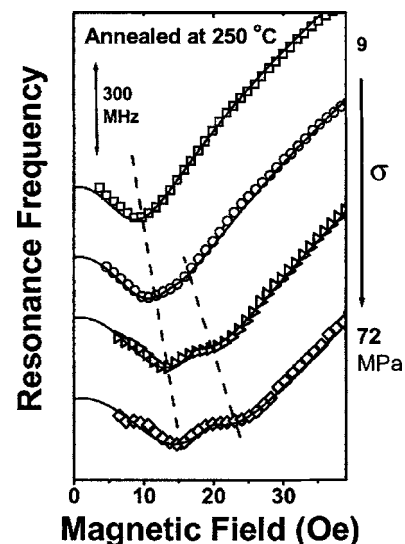


FIG. 6. FMR dispersion relation of the sample annealed at 250 °C with applied stress. The symbols ( $\square$ ) 9, ( $\circ$ ) 36, ( $\triangle$ ) 54, and ( $\diamond$ ) 72 MPa represent the experimental data, and the curves are the corresponding fittings. The dashed lines roughly accompany the anisotropy fields.

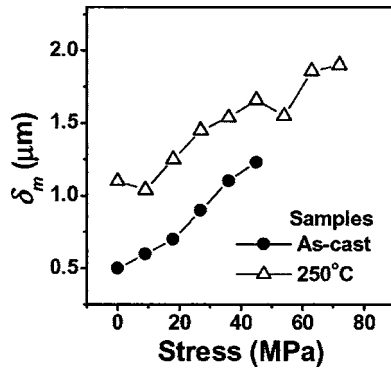


FIG. 7. Skin depth ( $\delta_m$ ) values for the as-cast and annealed samples at different stress conditions. The values were calculated at  $H=0$  and at the respective ferromagnetic resonance frequency.

increases with both the annealing temperature and applied stress. The increase in  $\delta_m$ , as well as the observed decrease of the MI ratio with applied stress (Fig. 3) is due to a decrease of the transverse permeability, as already reported in the literature (see, e.g., Ref. 1).

The annealing and the applied stress modify the wire's internal stress, which results in modifications of the magnetic anisotropy. For a glass-covered amorphous microwire, the magnetoelastic energy determines the domain structure and plays the major role in the magnetic behavior. Even for the studied wires (with vanishing magnetostriction), this is true due to the high induced and frozen stress levels associated to the fabrication process. In Ref. 10 a model explaining the wire's stress distribution has been proposed. The model takes into consideration the fact that the stress arises during wire solidification as a consequence of the difference between the thermal-expansion coefficients of the metal core and the glass cover, as well as due to the mechanical drawing in the preparation process. In this case, two regions can be identified: (i) an internal volume, where the axial stress component is the highest and positive, and (ii) an external volume, in which the circumferential stress component is the highest and negative. This stress configuration, associated to the negative sign of the magnetostriction, would give rise to a cylindrical IC with a radial anisotropy and an OS with a circumferential magnetization. Based on the calculations of the internal stress distribution applied to a sample with similar characteristics, one of the authors (Chiriac *et al.*<sup>11</sup>) found that the OS thickness would be around  $0.7 \mu\text{m}$ , which means that 90% of the sample's volume would be occupied by the IC.

By considering the magnetization, MI and FMR measurements presented in Figs. 2, 3(a), and 4, respectively, it can be concluded that in the absence of applied stress, the as-cast and the annealed samples do not show the above-described domain configuration. The domain structure that can be inferred from these curves, however, corresponds to a wire with a longitudinally magnetized IC, with essentially no OS contribution to the magnetization process.

The skin depths of the studied samples, without applied stress, are in the range of  $0.5 \leq \delta_m \leq 1 \mu\text{m}$  (see Fig. 7). The presence of a longitudinally magnetized IC can be explained in view of the high demagnetizing energy, which would arise

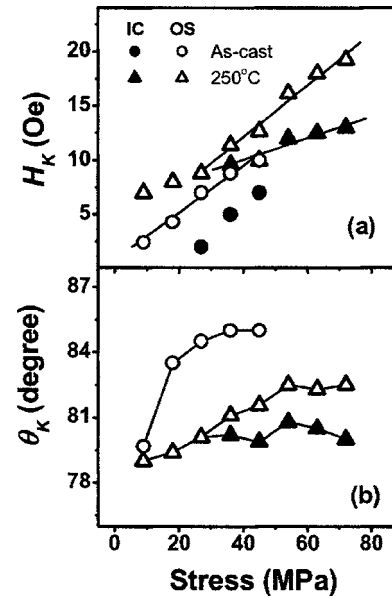


FIG. 8. Anisotropy field ( $H_K$ ) and anisotropy angle ( $\theta_K$ ) as function of the applied stress. The straight lines in panel (a) are linear fits to the experimental data, and the lines in panel (b) are only guides to the eye. (●) represents the data relative to the inner core. (○) represents the data relative to the OS. (△) and (▲) represent the outer and inner portions of the OS, respectively.

from a radially oriented domain structure, and/or due to a different stress distribution as compared with that reported in Ref. 10. This explains why the OS signature is not clearly observed in the magnetization loops. On the other hand, the circumferential character of the OS should be detected in both MI and the FMR measurements as the OS and  $\delta_m$  thickness are of the same order of magnitude. A further evidence for the nonexistence of the OS structure in nonstressed samples is the fact that the interface between IC and OS requires a transition region for the magnetic moments, like in a domain wall (DW).<sup>12</sup> This DW-like structure would have a thickness ( $\delta_w$ ) of

$$\delta_w \approx \sqrt{A/K}, \quad (2)$$

where  $A$  [ $=5 \times 10^{-12} \text{ J/m}$  (Ref. 13)] is the exchange constant and  $K$  ( $=130 \text{ J/m}^3$ ) the effective anisotropy energy density (extrapolated from Fig. 8 by fitting the FMR dispersion relation, as, discussed below). Expression (2) would give  $\delta_w \sim 0.3 \mu\text{m}$ , a value very close to the OS thickness ( $0.7 \mu\text{m}$  calculated in Ref. 11). Therefore, according to this evidence, the circularly magnetized OS probably is not present in the samples without stress.

When external stress is applied to the microwires, the internal stress distribution is changed, thus modifying the thickness of IC and OS. In a first approximation, based on the sample's volume conservation, while the axial stress component adds a positive value due to the contribution from the external stress (meaning a tensile stress), the radial and the circumferential components add a negative value (meaning a compressive stress). By considering the negative sign of the magnetostriction, the increase of these stress components emphasizes the transverse (circumferential) anisotropy of the OS, whose signature can be clearly seen in the MI and FMR dispersion relation curves [Figs. 3(b), 5, and 6]. The

increase in the transverse anisotropy energy also promotes a reduction in the thickness of the DW-like structure established between the IC and OS.

The FMR dispersion relation curves were fitted using FMR models as described in more detail in Refs. 4 and 9. In a few words, the magnetic system was considered as composed of two noninteracting magnetic layers. The energy components for each of the two layers were the Zeeman, demagnetizing, and uniaxial anisotropies. The energy was numerically minimized in order to find the equilibrium position of magnetization. The procedure followed the Smit and Beljers<sup>8</sup> work in which the roots of the determinant of a  $4 \times 4$  matrix, involving the second derivatives of the free energy with respect to the equilibrium angles of the magnetization, gives the dispersion relation of the system. Five parameters were used to fit the experimental curve:  $H_{K1}$ , and  $H_{K2}$ ;  $\theta_{K1}$  and  $\theta_{K2}$ , i.e., the angles between the  $i$ th easy axis (associated to  $H_{Ki}$ ,  $i=1, 2$ ) and the wire axis; and the spontaneous magnetization value  $M_S$  (same for both layers).

The above procedure was applied to the FMR dispersion relation obtained for the studied samples and under different applied stress. The fitted curves are shown as solid lines over the experimental data presented in Figs. 5 and 6 for the samples as cast and annealed at 250 °C, respectively. The fitting parameters ( $H_{K1}$ ,  $H_{K2}$ ,  $\theta_{K1}$ , and  $\theta_{K2}$ ) are shown in Fig. 8. There, the circles stand for the as-cast sample while the triangles are for the samples annealed at 250 °C. The open and solid symbols represent parameters relative to the external and internal layers respectively. The fitted  $\theta_K$  relative to the IC of the as-cast sample was considered zero (longitudinal) and, for clarity, it is not shown in panel (b) of Fig. 8.

As  $\sigma$  is applied to the as-cast sample,  $H_K (=K/2M_S)$  increases and, therefore, the  $\delta_w$  decreases as stated by the expression (2). Figure 7 shows that  $\delta_m$  also increases as  $\sigma$  is increased. In this way, the IC, beyond the OS, is also probed by the ac current, so the IC gives its contribution to the FMR dispersion relation. This contribution is responsible for the initial increase of the resonance frequencies (from 0 to  $\sim 5$  Oe, Fig. 5).

From the linear relation between  $H_K$  and  $\sigma$  observed in Fig. 8(a), and assuming that the only contribution to the anisotropy comes from the magnetoelastic energy, the magnetostriction was calculated as  $\lambda = -0.5 \times 10^{-7}$  for the as-cast sample. It is interesting to observe that as  $\sigma$  is increased, both fitting parameters  $H_K$  and  $\theta_K$  increase. This is an evidence of the transverse anisotropy improvement as  $\sigma$  is increased. It is worth to note that the  $H_K (=2.4$  Oe) value found for the as-cast sample with the lowest applied stress (9 MPa) is very close to that calculated in Ref. 11 ( $H_K = 2.2$  Oe), based on the internal stress distribution.

The most interesting result was obtained for the sample annealed at 250 °C. Two clear anisotropy fields can be observed, as depicted by the dashed lines in Fig. 6. The corresponding FMR dispersion relations were fitted considering that the OS of the studied sample is divided into two magnetic layers, each with its own  $H_K$  and  $\theta_K$ . The fits show that these layers have an almost circumferential anisotropy and that the division is effectively detected for stress higher than 35 MPa. Once again, this behavior can be explained in terms

of the skin depth and stress distribution in the wire. In other words,  $\delta_m$  increases with  $\sigma$ , so the probed volume is larger and the increase of  $H_K$  with  $\sigma$  results in a thicker OS with an associated thinner  $\delta_w$ . The external layer of the OS, represented by the open triangles in Fig. 8, exhibits higher  $H_K$  and  $\theta_K$  values when compared to the internal one, which is represented by the solid triangles. The proximity with the longitudinal IC can explain this difference, i.e., the coupling of the OS with the longitudinally magnetized IC could act to retain this portion of the OS. Melo *et al.*<sup>13</sup> have suggested such a kind of coupling. The application of  $\sigma$  reinforces the transversal character of the anisotropy, as observed in the as-cast sample. The difference in  $\theta_K$  for the two OS regions is also responsible for the peak structure in the MI curves shown in Fig. 3(b). These could be considered as a superposition of two peaks: the first one exhibits a smaller amplitude and a larger width when compared to the second one, which is sharper and has a higher amplitude. Each peak is associated to one of the OS layers. These differences on the peak structure can be understood as a consequence of the respective  $\theta_K$  values. The closer  $\theta_K$  is to 90° the sharper the corresponding peak will be.<sup>14,15</sup>

The magnetostriction values, extracted from the  $H_K \times \sigma$  curves for the sample annealed at 250 °C, are  $-0.5 \times 10^{-7}$  and  $-0.2 \times 10^{-7}$  for the external and internal OS, respectively. This difference in the  $\lambda_S$  values is not surprising, since the macroscopic magnetostriction of a ferromagnetic sample can be either the same defined value at each atomic site or the average of the local coefficients (see, e.g., Ref. 16). The latter is most plausible for the studied samples as the difference in the local stress level can easily produce differences in the local  $\lambda_S$  values.<sup>17</sup>

## V. CONCLUSIONS

The magnetic structure of glass-covered amorphous microwires with a slightly negative magnetostriction was studied by MI and MI-based FMR measurements. The samples were first annealed by Joule heating and then submitted to an external stress up to 80 MPa. Substantial differences between the magnetic structures of the samples with and without external stress, such as the presence of an outer-shell structure in the stressed samples only, were observed. In the case of the as-cast sample, as a consequence of the skin depth value, both the longitudinally magnetized IC and circumferentially magnetized OS were probed by the ac current resulting in the FMR dispersion relations shown in Fig. 6. This feature was confirmed by appropriate fitting of the FMR dispersion relation by using a phenomenological model. For  $\sigma > 35$  MPa, the sample annealed at 250 °C exhibited its outer shell divided into two layers, each one with a distinct anisotropy field and orientation relative to the wire's axis.

## ACKNOWLEDGMENTS

This work was partially supported by the Brazilian agencies, CNPq (Conselho Nacional de Desenvolvimento Científico e Tecnológico), CAPES (Coordenação de Aperfeiçoamento de Pessoal de Nível Superior), and FAPERGS (Fundação de Amparo à Pesquisa do Rio Grande do Sul).

- <sup>1</sup>H. Chiriac and T. A. Óvári, *Prog. Mater. Sci.* **40**, 333 (1996).
- <sup>2</sup>D. Ménard, D. Frankland, P. Ciureanu, and A. Yelon, *J. Appl. Phys.* **83**, 6566 (1998).
- <sup>3</sup>M. Carara, M. N. Baibich, and R. L. Sommer, *J. Appl. Phys.* **88**, 331 (2000).
- <sup>4</sup>R. B. da Silva, M. Carara, A. M. H. de Andrade, A. M. Severino, and R. L. Sommer, *J. Appl. Phys.* **94**, 4539 (2003).
- <sup>5</sup>H. Chiriac, M. Knobel, and T. A. Óvári, *Mater. Sci. Forum* **302-302**, 239, (1999).
- <sup>6</sup>L. Kraus, M. Knobel, S. N. Kane, and H. Chiriac, *J. Appl. Phys.* **85**, 5435 (1999).
- <sup>7</sup>V. Zhukova, A. F. Cobeño, A. Zhukov, J. M. Blanco, S. Puerta, J. Gonzalez, and M. Vázquez, *J. Non-Cryst. Solids* **287**, 31 (2001).
- <sup>8</sup>J. Smit and H. G. Beljers, *Philips Res. Rep.* **10**, 113 (1955).
- <sup>9</sup>J. Geshev, L. G. Pereira, and J. E. Schmidt, *Physica B* **320**, 169 (2002).
- <sup>10</sup>H. Chiriac, T.-A. Óvari, and Gh. Pop, *Phys. Rev. B* **52**, 10104 (1995).
- <sup>11</sup>H. Chiriac, T.-A. Óvari, and A. Zhukov, *J. Magn. Magn. Mater.* **254-255**, 469 (2003).
- <sup>12</sup>N. Usov, A. Antonov, A. Dykhne, and A. Lagar'kov, *J. Phys.: Condens. Matter* **10**, 2453 (1998).
- <sup>13</sup>L. G. C. Melo, D. Ménard, P. Ciureanu, A. Yelon, and R. W. Cochrane, *J. Appl. Phys.* **95**, 1331 (2004).
- <sup>14</sup>L. V. Panina, K. Mohri, T. Uchiyama, M. Noda, and K. Bushida, *IEEE Trans. Magn.* **31**, 1249 (1995).
- <sup>15</sup>L. Kraus, *J. Magn. Magn. Mater.* **195**, 764 (1999).
- <sup>16</sup>H. Chiriac, M. Negu, M. Vazquez, T. A. Ovari, and E. Hristoforou, *J. Magn. Magn. Mater.* **249**, 122 (2002).
- <sup>17</sup>A. Hernando, M. Vazquez, G. Rivero, J. M. Barandirán, O. V. Nielsen, and A. Garcia Escorial, *J. Phys.: Condens. Matter* **2**, 1885 (1990).